JOURNAL OF MATERIALS SCIENCE 26 (1991) 2501–2506

Characterization and metastability of alkoxy-derived tetragonal zirconia powder

HUEY-CHANG WANG, KWANG-LUNG LIN
Department of Materials Engineering, National Cheng Kung University, Tainan, 70101 Taiwan

The zirconia powders were synthesized through the hydrolysis of zirconium *n*-butoxides with air moisture as well as with aqueous solutions of different pH values to investigate the metastability of tetragonal (t)-ZrO_2. The SEM and TEM observations reveal that powders prepared with air moisture hydrolysis consist of spherical particles of 0.5–3.5 μm diameter, while gel-like powders composed of finer particles were obtained with aqueous solution hydrolysis. The samples obtained show different crystallization and tetragonal/monoclinic transformation temperatures on differential thermal analysis. The metastability of t-ZrO_2, investigated in terms of relative content with X-ray diffraction, was not explicable through the crystallite size effect. Instead, the existence of unpaired electrons, detected using electron paramagnetic resonance, and the strain within the powders, were found to be probably influential in affecting the metastability of t-ZrO_2.

1. Introduction

Since the existence of metastable tetragonal zirconia at room temperature was reported by Ruff and Ebert [1] and Clark and Reynolds [2], a great deal of work has been devoted to related studies [3–19]. Cypre's *et al.* [3], and others [4, 5] have attributed the stabilization of the tetragonal zirconia to OH^-, SO_4^{2-}, and other anionic impurities, whereas Garvie [6, 7] ascribed the phenomenon to the lower surface energy of the tetragonal (t) phase relative to that of the monoclinic (m) phase. Garvie reported that the crystallite size must be ≤ 30 nm for stabilizing the tetragonal phase. Livage *et al.* [11] and Murase *et al.* [12] considered the stabilization of the tetragonal phase to be related to the structural similarities between the amorphous and the tetragonal zirconia. Mitsuhashi *et al.* [13] proposed that the domain boundaries (strain energy) inhibit the t to m transformation; on the other hand, Murase and Kato [14] observed that water which exists during calcination enhanced the t to m transformation. Recently, Davis [15] and Srinivasan *et al.* [16] found that both the pH of the supernatant liquid and the time taken to attain this pH play dominant roles in determining the zirconia crystal phase; however, Torralvo *et al.* [17] and Osendi *et al.* [19] proposed that defect centres affect the metastability of the tetragonal phase.

In the above mentioned studies, thermal decomposition of amorphous hydrous zirconia, zirconium salts, ball milling of monoclinic zirconia, hydrothermal reaction, and vapour-phase reactions were described for the preparation of the metastable tetragonal zirconia. In addition, there are some reports of studies of the metastability of tetragonal zirconia powder synthesized through the thermal decomposition [8, 20] and controlled hydrolysis [21–23] of zirconium alkoxides. Yet, the mechanism for the existence of the metastable tetragonal phase of the alkoxy-derived zirconia powders at room temperature has been rarely discussed. We have tried in the present work, to investigate the metastability of zirconia powders synthesized through the hydrolysis of zirconium alkoxides under an uncontrolled atmosphere [24].

2. Experimental procedure

2.1. Powder synthesis

The alkoxy-derived zirconia powders were prepared through the hydrolytic polycondensation [24] of zirconium *n*-butoxide solution (0.2 M) which was synthesized by the reaction of $ZrCl_4$ with *n*-butanol [25]. The hydrolytic polycondensation of the $Zr(OBu)_4$ solution obtained was performed in two ways. First, aqueous solutions (100 ml) of desired pH, adjusted with HCl and NH_4OH, were dropped slowly into the $Zr(OBu)_4$ solution (100 ml); the resulting products were labelled G, because after drying at 65 °C for 18 h these products were gelatinous. For the second case, the $Zr(OBu)_4$ solutions (100 ml) were exposed to air moisture under ambient conditions for about 1 month; the resulting products were labelled P, because these products after drying were powdery.

2.2. Heat treatment and measurement

The differential thermal analysis (DTA) results were obtained by heating the dried samples at 10 °C min^{-1} to 1300 °C in air. The samples were cooled to room temperature at the same rate.

The dried zirconia powders were heated in a muffle furnace at a heating rate of 10 °C min^{-1} up to the desired temperature (350–800 °C). The samples were

0022–2461/91 $03.00 + .12

then either aged for 24 h at the final temperatures, or allowed to cool in the furnace. Some of the as-dried samples were pelletized at 30×10^3 p.s.i. before heating.

The calcined samples were examined by X-ray powder diffractometry (XRD) with Ni-filtered Cu radiation for phase characterization. Scanning electron microscopy (SEM) as well as transmission electron microscopy (TEM) were applied to investigate powder morphologies and electron diffraction patterns. The electron paramagnetic resonance (EPR) working in the X-band with α,α′-diphenyl-β-picrylhydrazyl (DPPH) as a standard was applied for studying the existence of unpaired electrons. BET measurements for surface-area studies were conducted using nitrogen adsorption at liquid nitrogen temperature.

The crystallite sizes were calculated using the $(1\,1\,1)_m$ and $(1\,1\,1)_t$ diffraction peaks from the Scherrer formula [26] with $D_{hkl} = 0.89\ \lambda\ (\beta_{hkl} \cos\theta)^{-1}$, where D_{hkl} is the crystallite size, λ is the radiation wavelength (Cu$K\alpha$). The corrected half-width, β_{hkl}, was obtained by using the (1 0 1) peak of low quartz as the standard for the Warren formula [26]. The half-width of the diffraction peak was obtained precisely by chart-recording at a scanning speed of 0.25 (2θ) min^{-1}. The tetragonal ZrO_2 content was estimated from the intensity relationship: $I(1\,1\,1)_t/I(1\,1\,\bar{1})_m + I(1\,1\,1)_t + I(1\,1\,1)_m$. The strain of the metastable tetragonal ZrO_2 was estimated from Hall's equation [13] from the $(1\,1\,1)_t$ and $(2\,2\,2)_t$ reflections

$$(\beta_{hkl} \cos\theta)/\lambda = 1/D^{\circ}_{hkl} + \eta_{hkl}(\sin\theta/\lambda) \quad (1)$$

where D°_{hkl} denotes the effective crystallite size in the $\langle h\,k\,l \rangle$ direction and η_{hkl} denotes the strain in that direction.

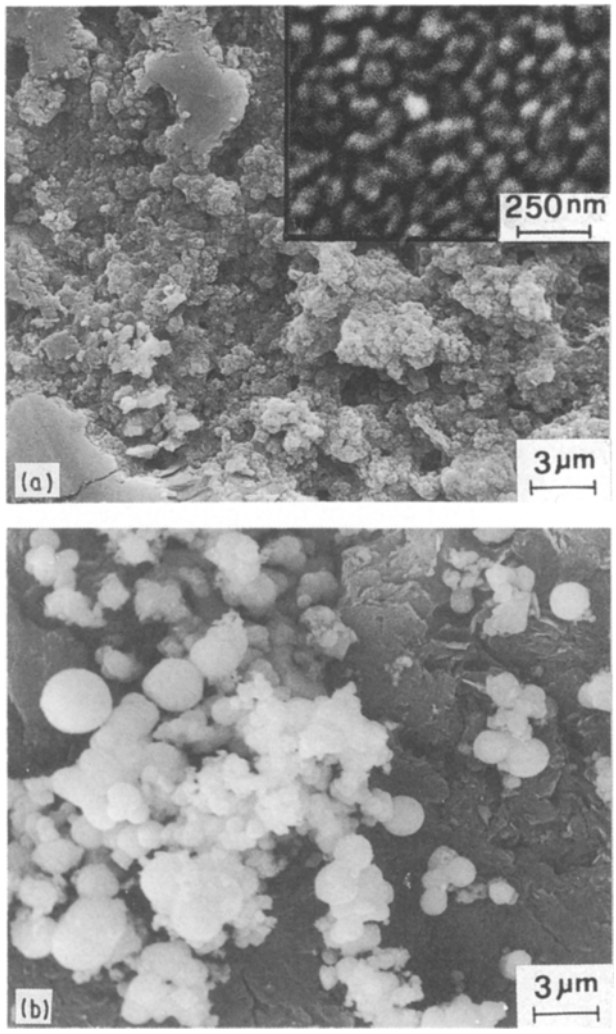

Figure 1 Scanning electron micrographs of (a) sample G, (b) sample P, dried at 65 °C for 18 h.

3. Results and discussion

3.1. Characteristics of alkoxy-derived zirconia

The microstructural morphologies of samples G and P are shown in Fig. 1a and b, respectively. The morphologies of samples G and P are quite different. The particles of sample G were closely aggregated, and the aggregates seemed to be composed of particles ranging from 40–60 nm diameter. However, the particles of sample P were of spherical agglomerates with diameters ranging from 0.5–3.5 μm. Additionally, the bright-field and dark-field TEM images of sample G as shown in Fig. 2a and b, respectively, show that the aggregated particles of sample G are composed of crystallites smaller than 45 nm; i.e. the crystallites have different dimensions from those of the particles observed in Fig. 1. Meanwhile, the BET values of samples P and G, dried at 200 °C, are 82 ± 10 and 133 ± 10 $m^2\ g^{-1}$, respectively, which correspond to the d_{BET} of 12 ± 0.2 and 7.4 ± 0.2 nm, respectively. A comparison of these d_{BET} with the dimensions of the particles observed by SEM and TEM indicates that both sample P and sample G are actually composed of much finer particles (domains) or crystallites than the particles observed by SEM and TEM [13].

The selected-area electron diffraction (SAD) pattern of the as-dried sample G is shown in Fig. 2c. This SAD pattern indicates that sample G exhibits a certain degree of crystallinity even before calcination. The structure derived from the ring diffraction pattern is very close to that of the tetragonal phase. This result could be explained as the reason why the amorphous alkoxy-derived precursor, detected by XRD, can easily crystallize to the metastable tetragonal phase, as proposed by others [11, 12].

3.2. Thermal evolution

The DTA curves of samples P and G prepared by hydrolysis with solutions of various pH are shown in Fig. 3. The curves exhibit broad dehydration endothermal peaks at ≃ 90 °C, and the endothermal peaks of the sample G are stronger than those of sample P. Additionally, the DTA curves of sample P also show a broad exothermal peak at ≃ 280 °C, which is caused by the decomposition and burning of bonding alkoxy groups [8, 27]. Meanwhile, G samples prepared with solutions of higher pH values also exhibited stronger intensities for this peak. Bradley and Carter [28] observed that the products synthesized by the hydrolysis of some primary zirconium alkoxides were polymerized oxide–alkoxides $[ZrO_x(OR)_{4-2x}]_n$, and it was also shown [29] that the

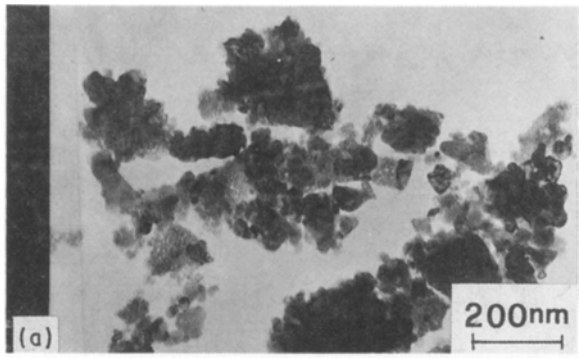

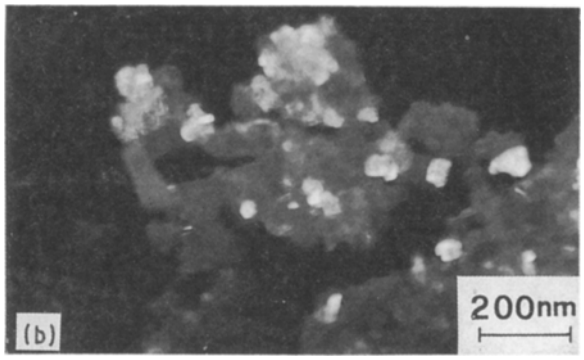

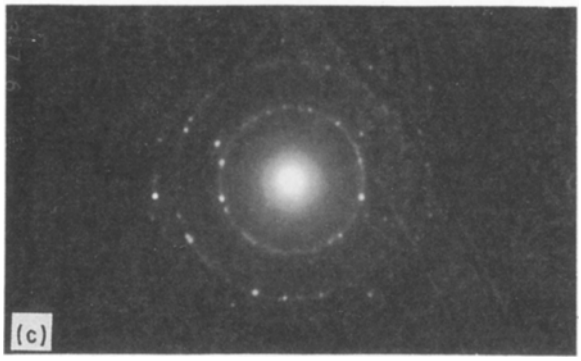

Figure 2 Transmission electron micrographs of sample G: (a) bright field, (b) dark field, (c) SAD; dried at 65 °C for 18 h.

OH^- ions in the hydrolysis medium would increase the rate of the polycondensation reaction. The DTA results of the present work suggest that samples P and G prepared with solutions of higher pH values contain more residual alkoxy groups, which do not react completely with H_2O.

On the other hand, the DTA curves of all of the samples show sharp exothermal glow peaks at 411–436 °C, which have also been identified as the crystallization temperatures of t-ZrO_2 [11, 27]. Besides the crystallization peaks, two additional small peaks were also observed, but as yet the origin of these peaks is not understood. The crystallization temperatures of the amorphous precursor phase and the transition temperatures of the high-temperature tetragonal to monoclinic transition for samples P and G are summarized in Table I. It is seen that the crystallization temperatures increase with the pH of the aqueous solutions, and sample P exhibits the highest crystallization temperature. In view of the contents of the alkoxy groups, this suggests that the existence of alkoxy groups tends to inhibit crystallization, i.e. to raise the crystallization temperatures. The temperatures of the t to m phase transformation decrease with increasing pH values. However, Maiti *et al.* [30] reported that the temperatures of the t to m phase transformation decrease with decreasing crystallite size of t-ZrO_2, and Whitney proposed [31] that the increase in external pressure tends to lower this phase transformation temperature. Therefore, G samples obtained from aqueous solutions of higher pH values probably have smaller crystallite sizes of the high-temperature t-ZrO_2, or exhibit higher strain among the crystallites.

TABLE I Temperatures of crystallization and of high-temperature t-ZrO_2

Samples	Crystallization temperature (°C)[a]	Transformation temperature (°C)[a]
pH 1	411	924
pH 3	412	888
pH 6	412	884
pH 9	416	866
pH 11	422	843
Sample P	436	871

[a] Measured from DTA.

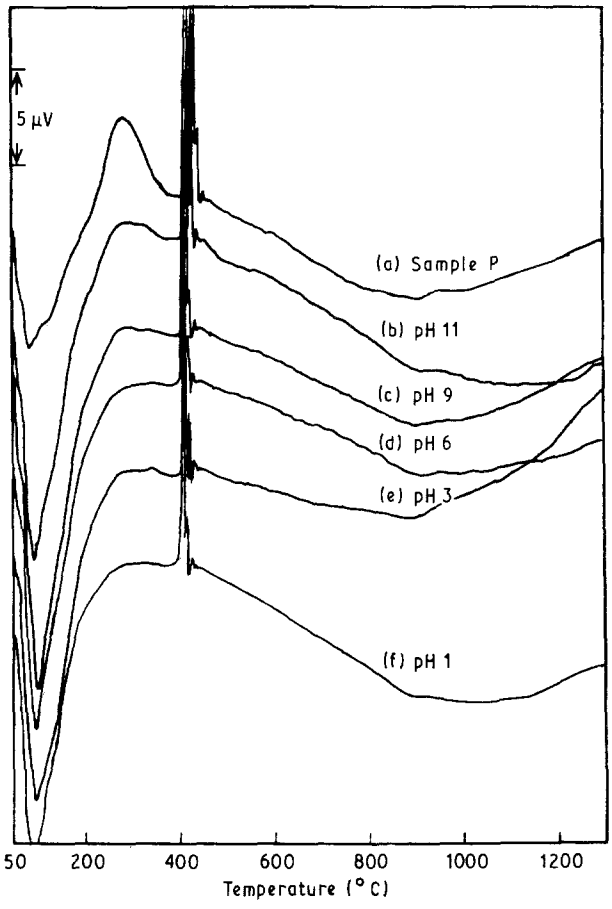

Figure 3 DTA curves of (a) sample P, and sample G obtained with (b) pH 11, (c) pH 9, (d) pH 6, (e) pH 3, (f) pH 1, aqueous solutions.

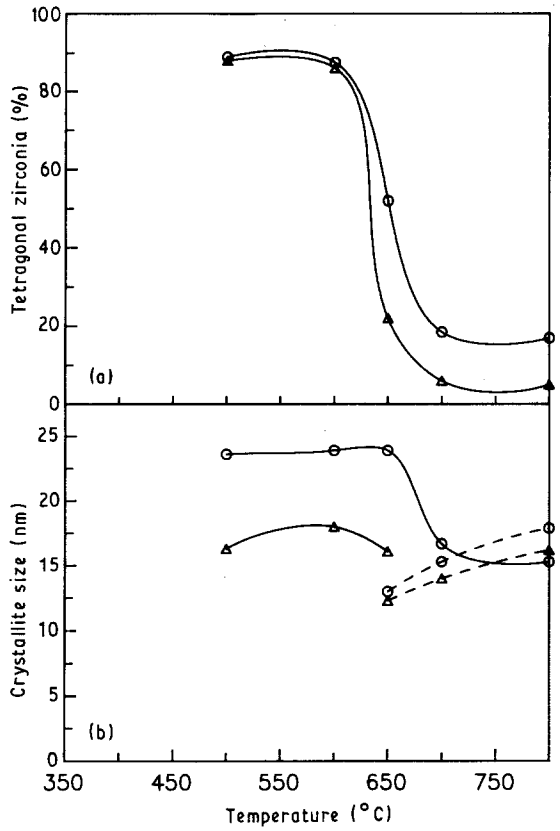

Figure 4 (a) Relative t-ZrO_2 content, (b) crystallite size, of samples (○) P and (△) G (pH 6) heated to various temperatures. (——) Tetragonal, (– – –) monoclinic; furnace cooled.

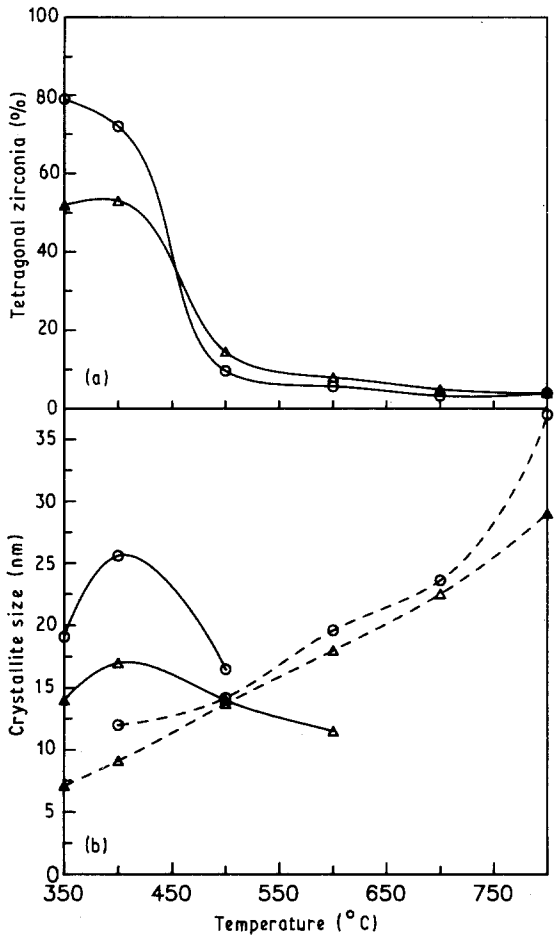

Figure 5 (a) Relative t-ZrO_2 content, (b) crystallite size, of samples (○) P and (△) G (pH 6) heated to various temperatures for 24 h, and furnace cooled. (——) Tetragonal, (– – –) monoclinic.

3.3. The metastability of t-ZrO_2

The relative t-ZrO_2 content and the crystallite sizes of samples P and G are shown in Fig. 4a and b, respectively. The results shown in Fig. 4a indicate that the t to m phase transformation takes place apparently between 600 and 700 °C. The relative content of t-ZrO_2 of sample P is always greater than that of sample G. However, Fig. 4b shows that the crystallite sizes of tetragonal and monoclinic ZrO_2 of sample P are larger than those of sample G, especially for the case of the tetragonal phase. This result is not as the crystallite size effect [6, 7] predicts. Meanwhile, the monoclinic crystallite size of ZrO_2 is also smaller than 30 nm, which is the critical crystallite size of metastable t-ZrO_2 suggested by Garvie [6, 7]. In addition the relative content of t-ZrO_2 and the crystallite sizes of both samples heated for 24 h at certain temperatures are shown in Fig. 5. Sample P also contains more t-ZrO_2 than sample G. Yet, sample G possesses smaller crystallite sizes when heat treated at 350 and 400 °C. Other results are generally similar to the results of Fig. 4.

On the other hand, the relative t-ZrO_2 content and the crystallite size of G samples hydrolysed with solutions of various pH are shown in Fig. 6. The results shown in Fig. 6a indicate that the relative t-ZrO_2 content seems to be independent of the pH value of the aqueous solution, although the G samples prepared with pH 1 aqueous solution have a smaller crystallite size. Fig. 7 shows the results of the samples heat treated for 24 h, the relative content and the crystallite size of t-ZrO_2 basically increase with pH of the aqueous solutions, especially at lower temperatures. Sim-

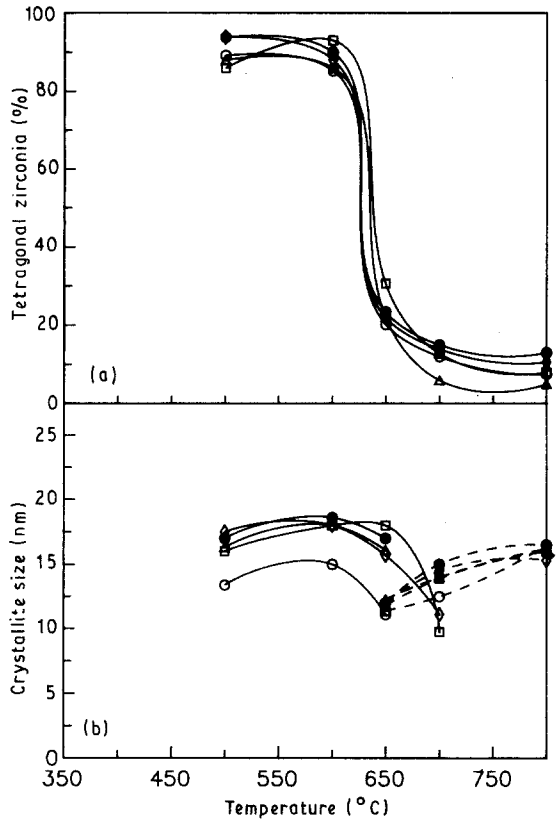

Figure 6 (a) Relative t-ZrO_2 content, (b) crystallite size, of sample G hydrolysed with solutions of various pH, heated to various temperatures, and furnace cooled. pH: (●) 11, (◇) 9, (△) 6, (□) 3, (○) 1. (——) Tetragonal, (– – –) monoclinic.

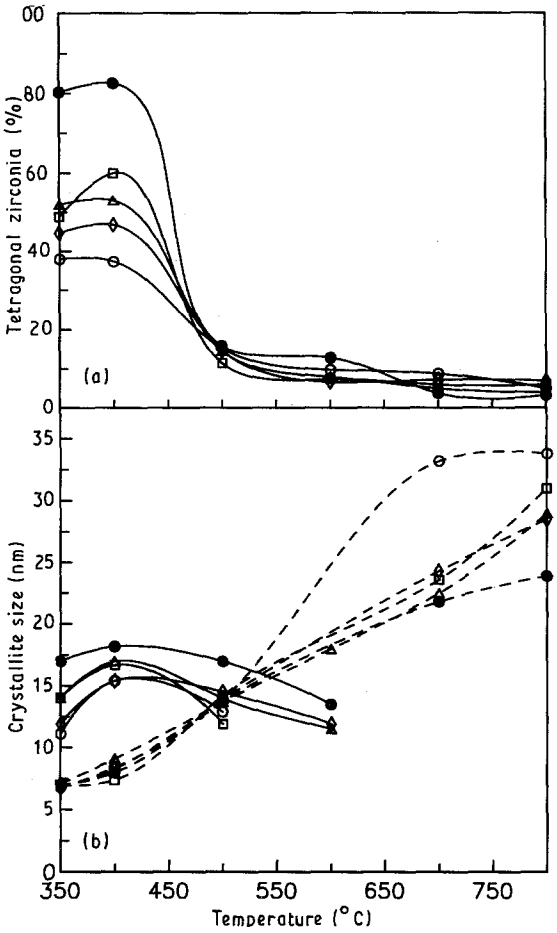

Figure 7 (a) Relative t-ZrO_2 content, (b) crystallite size, of sample G hydrolysed with solutions of various pH, heated to various temperatures for 24 h, and furnace cooled. See Fig. 6 for legend.

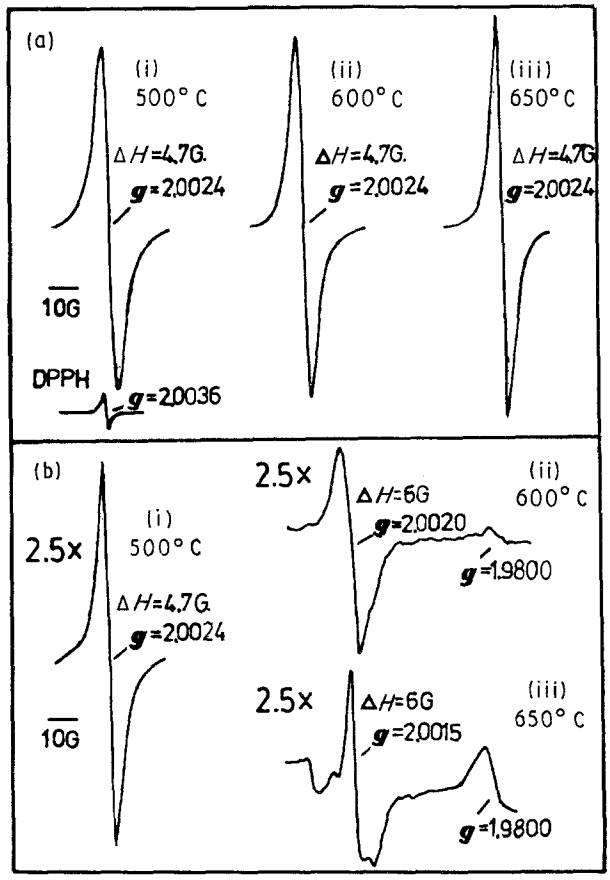

Figure 8 EPR spectra of (a) sample P, (b) sample G heated to (i) 500 °C, (ii) 600 °C, (iii) 650 °C.

ilar to the results shown by Figs 4 and 5, the results of Fig. 7 do not correspond to a crystallite size effect as described by Garvie [6, 7]. On the contrary, the monoclinic crystallite size seems to decrease with the pH of the aqueous solution.

The EPR spectra of samples P and G which were heat treated at 500, 600 and 650 °C are shown in Fig. 8a and b, respectively. Sample P shows slightly asymmetrical EPR signal with $g = 2.0024 \simeq g_e$ and $\Delta H = 4.7$ G. The intensities, g values, and ΔH do not show any significant changes with respect to increasing temperatures. This signal has been identified as corresponding to unpaired electrons in the oxygen vacancies [17–19] or residual carbon impurities [32]. On the contrary, the signals of sample G shown in Fig. 8b show a significant change. In Fig. 8b(ii), the intensities of sample G decrease after having been heat treated at 600 °C. There exists a broad signal with $g = 2.0020$, $\Delta H = 6$ G, and a small signal with $g = 1.9800 < g_e$, and the latter has been ascribed [33] to Zr^{3+}. When sample G was heated to 650 °C, the intensity of the signal with $g = 1.9800$ increases (Fig. 8b(iii)). A comparison of the intensity variation of the signals $g = 2.0024$, Fig. 8, and the relative content of t-ZrO_2, Fig. 4a, does not show any parallel correlation. Accordingly, the stability of the metastable phase observed in the present work cannot be explained adequately simply based on the existence of oxygen vacancies or carbon impurities which trap unpaired electrons in the bulk of the samples.

The relative t-ZrO_2 content and crystallite size of some pelletized samples which have been heat treated at 350 °C for 24 h are summarized in Table II. A comparison of the relative contents of t-ZrO_2 shows that the pelletized samples have much more t-ZrO_2 content and larger tetragonal crystallite size than the powdery samples. Meanwhile, the t-ZrO_2 content of the pelletized samples seem to be less dependent on the pH values. The crystallite size variation with respect to tetragonal content observed in this case seems to correspond to the results of previous work [24], whereby the samples were pelletized at 45 $\times 10^3$ p.s.i. These results show that the external pressure, resulting in an internal strain existing among the domains, indeed can stabilize the t-ZrO_2. It is well established [29] that OH^- ions enhance the polycondensation reaction. Therefore, G samples obtained with aqueous solutions of higher pH values and

TABLE II The relative t-ZrO_2 content and crystallite size of powdery and pelletized samples heated at 350 °C for 24 h

	Powder		Pellets[a]	
Samples	Tetragonal (%)	d (nm)	Tetragonal (%)	d (nm)
pH 1	38	11.1	84	20.1
pH 3	49	13.0	96	18.9
pH 6	52	14.0	90	19.1
pH 9	45	11.9	93	20.4
pH 11	80	17.0	80	20.1
Sample P	79	19.1	90	23.6

[a] Pelletized at 30×10^3 p.s.i.

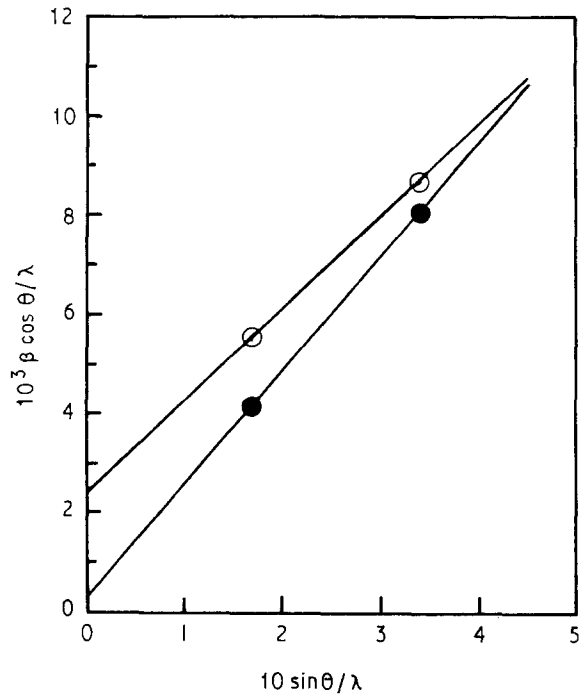

Figure 9 Crystallite size plotted versus strain for samples (●) P and (○) G (pH 6) heated to 500 °C for 24 h.

sample P possess larger strain, which may be dependent on the degree of hydrolytic polycondensation, resulting in a larger local network of oxides, inside the domains to stabilize t-ZrO_2.

The above results provide clues for the understanding of the t to m phase transformation route. If the metastability of t-ZrO_2 is based on the thermodynamic requirements, thermodynamically, the following relation governs the transformation behaviour [9]

$$(G_t - G_m) + (S_t\gamma_t - S_m\gamma_m) + (V_t - V_m) = 0 \quad (2)$$

where G, S, γ, and V denote the free energy, molar surface area, surface energy, and strain energy of the tetragonal or monoclinic phase, respectively. According to Equation 2, the stabilization of the tetragonal phase must be attributed to a negative surface energy or strain energy difference, because the first term is positive at room temperature. However, the crystallite size effect, i.e. the surface energy effect, is not found to be valid in the present work as delineated in Figs 4 and 5. Accordingly, the strain energy would dominantly contribute to the stabilization of t-ZrO_2. The relation between the effective crystallite size and the strain of t-ZrO_2 is shown in Fig. 9. As the results show, sample P exhibits a greater strain (2.3×10^{-2}) than sample G (1.8×10^{-2}), and this result corresponds to the explanation described above.

4. Conclusion

It has been shown that alkoxy zirconia with different characteristics could be prepared by the hydrolysis of $Zr(OBu)_4$ with air moisture as well as with aqueous solutions of different pH values. The samples obtained from air moisture and higher pH values would contain a larger content of t-ZrO_2, despite the larger crystallite size. The crystallite size and the existence of oxygen vacancies or carbon radicals are not strongly related to the content of t-ZrO_2. Therefore, the strain, which depends on the degree of hydrolytic polycondensation, within the crystallites (domains) would predominantly govern the metastability of the t-ZrO_2.

Acknowledgement

The financial support of the present work from the National Science Council of the Republic of China under NSC76-0405-E006-19 is gratefully acknowledged.

References

1. O. RUFF and F. EBERT, *Z. Anorg. u. Allgem. Chem.* **180** (1929) 19; *Ceram. Abstr.* **8** (1929) 660.
2. G. L. CLARK and D. H. REYNOLDS, *Ind. Eng. Chem.* **29** (1937) 711; *Ceram. Abstr.* **16** (1937) 259.
3. R. CYPRE'S, R. WOLLAST and J. RAUCQ, *Ber. Deut. Keram. Ges.* **40** (1963) 527.
4. A. CLEARFIELD, *Inorg. Chem.* **3** (1964) 146.
5. E. D. WHITNEY, *Trans. Faraday Soc.* **61** (1965) 1991.
6. R. C. GARVIE, *J. Phys. Chem.* **69** (1965) 1238.
7. *Idem, ibid.* **82** (1978) 218.
8. K. S. MAZDIYASNI, C. T. LYNCH and J. S. SMITH, *J. Amer. Ceram. Soc.* **48** (1965) 372.
9. J. E. BAILEY, D. LEWIS and L. J. PORTER, *Trans. J. Brit. Ceram. Soc.* **71** (1972) 25.
10. Y. SUYAMA, T. MIZOBE and A. KATO, *Ceram. Int.* **3** (1977) 141.
11. J. LIVAGE, K. DOI and C. MAZIERES, *J. Amer. Ceram. Soc.* **51** (1968) 349.
12. Y. MURASE, E. KATO and H. MATSUMOTO, *Nippon Kagaku Kaishi* **12** (1972) 2329.
13. T. MITSUHASHI, M. ICHIHARA and U. TATSUKE, *J. Amer. Ceram. Soc.* **57** (1974) 97.
14. Y. MURASE and E. KATO, *ibid.* **66** (1983) 196.
15. B. H. DAVIS, *ibid.* **67** (1984) C-168.
16. R. SRINIVASAN, M. B. HARRIS, S. F. SIMPSON, R. J. DEANGELIS and B. H. DAVIS, *J. Mater. Res.* **3** (1988) 787.
17. M. J. TORRALVO, J. SORIA, and M. A. ALARIO, in "Proceedings of the 9th International Symposium on the Reactivity of Solids", Cracow, 1980, pp. 306–400.
18. M. J. TORRALVO, M. A. ALARIO and J. SORIA, *J. Catal.* **86** (1984) 473.
19. M. I. OSENDI, J. S. MOYA, C. J. SERNA and J. SORIA, *J. Amer. Ceram. Soc.* **68** (1985) 135.
20. K. S. MAZDIYASNI, C. T. LYNCH and J. S. SMITH, *ibid.* **49** (1966) 286.
21. B. E. YOLDAS, *ibid.* **65** (1982) 387.
22. J. C. DEBSIKDAR, *J. Non-Cryst. Solid* **87** (1986) 343.
23. B. E. YOLDAS, *J. Mater. Sci.* **21** (1986) 1080.
24. K. L. LIN and H. C. WANG, *ibid.* **21** (1986) 1080.
25. D. C. BRADLEY and W. WARDLAW, *J. Chem. Soc.* **73** (1951) 280.
26. H. P. KLUG and L. E. ALEXANDER, "X-Ray Diffraction Procedures" (Wiley, New York, 1954) Ch. 9.
27. P. KUNDU, D. PAL and S. SEN, *J. Mater. Sci.* **23** (1988) 1539.
28. D. C. BRADLEY and D. G. CARTER, *Can. J. Chem.* **39** (1961) 1434.
29. M. PRASSAS and L. L. HENCH, in "Ultrastructure Processing of Ceramics, Glasses, and Composites", edited by L. Hench and D. Ulrich (Wiley, New York, 1984) pp. 100–25.
30. H. S. MAITI, K. V. G. K. GOKHALE and E. C. SUBBARAO, *J. Amer. Ceram. Soc.* **55** (1972) 317.
31. E. D. WHITNEY, *ibid.* **45** (1962) 612.
32. A. SAMDI, T. G. BARON, B. DURAND and M. ROUBIN, *Ann. Chim. Fr.* **13** (1988) 171.
33. V. S. VAINER, A. I. VEINGER, A. V. SHKUL'KOV and Y. A. POLONSKII, *Sov. Phys. Solid State* **20** (1978) 1628.

Received 23 January
and accepted 30 May 1990